A Model-Based Compressed Sensing Method for Fast Cardiac T1 Mapping in Small Animals

W. Li[1,2], M. Griswold[1,3], and X. Yu[1,3]

[1]Biomedical Engineering Department, Case Western Reserve University, Cleveland, OH, United States, [2]Case Center for Imaging Research, Case Western Reserve University, Cleveland, OH, United States, [3]Radiology Department, Case Western Reserve University

Introduction

Direct measurement of the longitudinal relaxation time T_1 provides objective and quantitative diagnostic information. However, current T_1 mapping methods are generally time consuming without the aid of fast imaging. The current study developed a model-based compressed sensing (CS) method for fast cardiac T_1 mapping in small animals. Based on the physics of magnetization recovery, the aliasing noises associated with under-sampling was removed by exploiting the sparsity of the signals in the T_1 recovery direction. Simulation and imaging studies on phantom and *in vivo* mouse were performed to evaluate the accuracy of different reconstruction approaches at various experimental conditions. Our results suggest that current CS method, when combined with saturation recovery Look-Locker method (SRLL) (1), allows fast (<80 s) T_1 mapping of the mouse heart at high spatial resolution (234x469 μm^2).

Methods

Model-Based Compressed Sensing For T_1 mapping using saturation recovery, the magnitude of a signal series (X) of an imaging pixel is related to a sparse transformed domain (γ) by the equation shown on the right. The transform matrix D (dictionary) comprises of columns (atoms) that describe the signal evolution related to specific T_1 values. Under-sampling of the k-space leads to aliased images with more than one nonzero coefficients in γ. However, the randomness of the under-sampling renders the coefficients associated with aliased pixels smaller than that of the original pixel. Sparsification of γ using the orthogonal matching pursuit (OMP) algorithm (2) can seek the atom with the largest correlation to the signal and thus removes the aliasing noise for accurate image reconstruction (3).

$$\begin{pmatrix} X_1 \\ \vdots \\ X_n \end{pmatrix} = D\gamma = \begin{pmatrix} 1-\exp(-t_1/T_{1,1}) & \cdots & 1-\exp(-t_1/T_{1,m}) \\ \vdots & \ddots & \vdots \\ 1-\exp(-t_n/T_{1,1}) & \cdots & 1-\exp(-t_n/T_{1,m}) \end{pmatrix} \begin{pmatrix} \gamma_1 \\ \vdots \\ \gamma_m \end{pmatrix}$$

Simulation and Phantom Studies Validation of the current method was first performed on a digital Shepp-Logan phantom with T_1 values ranging from 0.3 to 1.5 s. The impact of imaging resolution and acceleration factor (R) on reconstruction accuracy was evaluated. Further validation was performed using imaging data acquired from a phantom of $MnCl_2$ solution. Several reconstruction approaches that used pre-calculated phase maps were evaluated to account for phase variations caused by instrumentation noises. Specifically, pre-calculated phase maps were generated from the center 8 PE lines, a fully-sampled proton density (M_0) image and a separate fully-sampled SRLL dataset, respectively.

In Vivo Validation *In vivo* T_1 mapping of a mouse heart was performed on a horizontal 7T Bruker scanner. ECG-triggered SRLL images were acquired before, during, and after manganese infusion. The acquired MRI data were retrospectively under-sampled with an acceleration factor of 2. The model-based CS reconstruction was performed. The results were compared with that from the fully-sampled data.

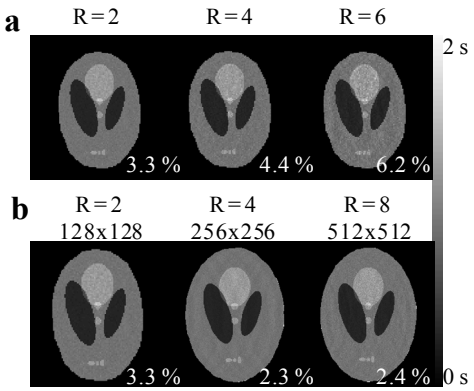

Figure 1. CS reconstructed T_1 maps with different acceleration factor (**a**) and matrix size (**b**).

Results

Results of simulation studies are shown in Fig. 1. At an SNR of 40, an acceleration factor of 2 led to accurate reconstruction with only 3.3% normalized root mean square error (NRMSE). Higher acceleration factor increased the reconstruction noise slightly. However, NRMSE remained <7% even with an acceleration factor of 6 (Fig. 1a). With a large matrix size, corresponding to the acquisition of images at high spatial resolution, a higher acceleration factor can be achieved without sacrificing the accuracy (Fig. 1b).

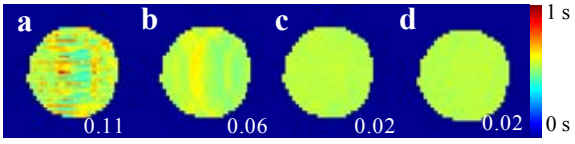

Figure 2. CS reconstructed T_1 maps without the use of phase maps **(a)** and using phase maps **(b)-(d)**. NRMSE at right bottom.

Fig.2 shows the reconstruction of under-sampled MRI data from a phantom. Significant error reduction was observed in reconstructed T_1 maps using pre-calculated phase maps. Since the sparsification transform was based on the signal model that only described the magnitude of signal recovery, aliasing noise in phase cannot be effectively removed and thus led to significant reconstruction errors (Fig. 2a). Using the low-resolution phase maps, the reconstruction error was greatly reduced, but aliasing artifacts remained noticeable (Fig. 2b). These artifacts were completely removed when more accurate phase maps were obtained from either the M_0 image or a separate fully-sampled SRLL dataset (Fig. 2c&d).

Fig. 3 shows the results from the *in vivo* MRI study. Accurate reconstruction was achieved at an acceleration factor of 2, leading to similar T_1 maps and mean T_1 values generated from the reconstructed and fully-sampled datasets (Fig. 3a&b). Similar reconstruction accuracy was also observed in the dynamic datasets throughout the dynamic imaging protocol.

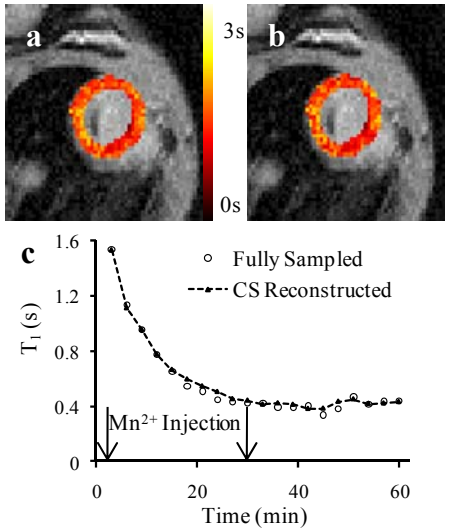

Figure 3. In vivo MEMRI study. **(a)&(b)**. T_1 maps from fully-sampled and CS-reconstructed images respectively. **(c)**. Time courses of T_1 changes.

Conclusion

The current model-based CS method showed the potential to greatly accelerate T_1 mapping under various experimental conditions. The use of pre-calculated phase maps from the fully-sampled M_0 image or a separate SRLL measurement accounted for the phase variations associated with field inhomogeneity and eddy current and thus significantly improved the reconstruction accuracy. The results from *in vivo* MEMRI study suggest that fast (<1.5 min) T_1 mapping of the mouse heart at high spatial resolution (234x469 μm^2) can be achieved with a combination of the SRLL and the current model-based CS methods.

References

1. Li W et al, MRM 2010.
2. Tropp et al, IEE Trans Form Theo, 2007.
3. Doneva et al, MRM 2010.